Scheme V

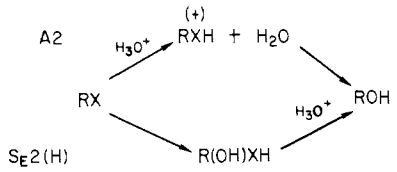

those of the weakly basic substrates discussed shows that relatively small changes in structure can lead to major changes in the kinetics form of the reaction in acid solution.

Relation between A2 and $S_E2(H)$ Mechanisms. The generally accepted A2 mechanism provides a reasonable model for many acid-catalyzed bimolecular hydrolyses,[20] but it fails for acid reactions of *N*-acylpyrroles and -indoles and probably for most of the reactions in Scheme IV. The mechanistic distinction depends on the timing of the addition of the hydrogen ion and water, and there should be a merging of the two mechanisms as the properties of the substrate change, e.g., going from a relatively basic amide to a readily hydrated acylpyrrole changes to mechanism from A2 (initial protonation) to $S_E2(H)$ (initial hydration).

For acid-catalyzed hydrolyses of a substrate, RX, the A2 and $S_E2(H)$ mechanisms can be represented as in Scheme V.

These reactions are drawn as stepwise processes, and it is reasonable that a relatively basic substrate should require activation to water attack by prior protonation, whereas the presence of strongly electron-withdrawing groups should favor hydration and require acid catalysis of conversion of the *gem*-diol into products.

Jencks[49] has discussed the relation between stepwise and concerted reactions and has pointed out that the latter avoid formation of high-energy intermediates, which is kinetically unfavorable.

These observations also suggest that it may be useful to reconsider bimolecular acid-catalyzed hydrolyses in terms of a spectrum of mechanisms depending on the timing of the various steps.

For example, acid hydrolyses or simple monoalkyl phosphates[35,50] have the kinetic form typical of water attack upon protonated substrate, whereas the acid hydrolyses of several aryl phosphates are relatively rapid but show rate maxima in acid. These "anomalous" hydrolyses have very negative entropies of activation and negative kinetics salt effects and show strong dependence on water activity. In addition, triaryl phosphates are very weak bases, so that their conjugate acids will be high-energy intermediates, which immediately suggests that hydrolysis will occur by a reaction path that avoids their formation. Thus there appear to be close similarities between these acid hydrolyses and those of the acyl pyrroles and indoles.

Hydrolyses of aryloxyphosphonium salts (**6**) can be regarded as models for attack of water upon a hypothetical protonated aryl phosphate (**7**).

$$\underset{\mathbf{6}}{MeP(OAr)^{3+}} \qquad \underset{\mathbf{7}}{(ArO)_3POH^+}$$

It is, however, difficult to reconcile the rate of hydrolysis of **6** with those of the acid hydrolyses of triaryl phosphates in terms of reaction between water and protonated substrate (**7**). But hydrolysis of **6** will be an inadequate model if acid hydrolysis of aryl phosphates does not occur by water attack upon protonated substrate.

For the acid hydrolysis of *N*-(trifluoroacetyl)pyrrole, the amide is in equilibrium with the *gem*-diol, and this is probably also true for hydrolyses of **2–4**. However, this is not the situation for several of the reactions shown in Scheme IV, if only because oxygen exchange between water and substrate is not observed, but the common feature is that they probably do not involve attack of water upon the protonated substrate even though this is the mechanism for hydrolysis of structurally similar but more basic substrates. In the acid hydrolysis of *N*-(trifluoroacetyl)pyrrole, the *gem*-diol is a low-energy species and its acid decomposition is rate limiting. For a simple aliphatic amide the conjugate acid is a low-energy species and its conversion to products with attack of water is rate limiting. Thus, with a systematic change of structure of an amide, it should be possible to change from one mechanism to another, possibly by reactions that involve concerted addition of water and proton transfer to the leaving group, and this possibility is being tested.

Acknowledgment. Support of this work by C.N.R. Rome, the National Science Foundation, and the North Atlantic Treaty Organization is gratefully acknowledged.

(49) W. P. Jencks, *Chem. Rev.*, **72**, 705 (1972).
(50) R. Kluger and F. H. Westheimer, *J. Am. Chem. Soc.*, 91, 4143 (1969).

Tridentate to Bidentate in a Platinum(II) Chelate: A 90° Anthranilaldehyde Rotation

Alan J. Jircitano, William G. Rohly, and Kristin Bowman Mertes*

Contribution from the Department of Chemistry, University of Kansas, Lawrence, Kansas 66045.
Received December 23, 1980

Abstract: The labilization of a coordinated formyl group in a platinum(II) chelate by nucleophilic ligands has been examined structurally. The chelating ligand is the deprotonated dimeric Schiff base condensate of *o*-aminobenzaldehyde. The aldehyde was trapped in its uncoordinated form by adding a 1:1 molar ratio of triphenylphosphine to the complex in acetonitrile. The resulting adduct crystallizes in the space group $C2/c$ with unit cell dimensions a = 32.75 (6) Å, b = 10.04 (2) Å, c = 19.71 (7) Å, and β = 118.5 (2)°. The immediate coordination sphere of the platinum consists of two nitrogens from the chelate, the phosphorus of the triphenylphosphine, and a chloride. The benzaldehyde ring, upon dissociation of the aldehyde oxygen from the platinum, has rotated 90° to a position perpendicular to the deprotonated *o*-aminobenzylidene group. The aldehyde oxygen is poised almost directly above the imine nitrogen at a distance of 2.87 (1) Å.

Introduction

The utility of transition metal ions in facilitating condensation reactions of organic substrates, particularly in the synthesis of macrocyclic ligands, is well documented. Unfortunately, the mechanistic details of many of these template reactions have been elusive. In order to elucidate mechanistic pathways and ultimately the role of the metal ion in these reactions, it is vital that the presence of postulated intermediates be verified. Many of the condensation reactions employed to yield macrocyclic products are of the Schiff base variety: the condensation of a carbonyl with

0002-7863/81/1503-4879$01.25/0

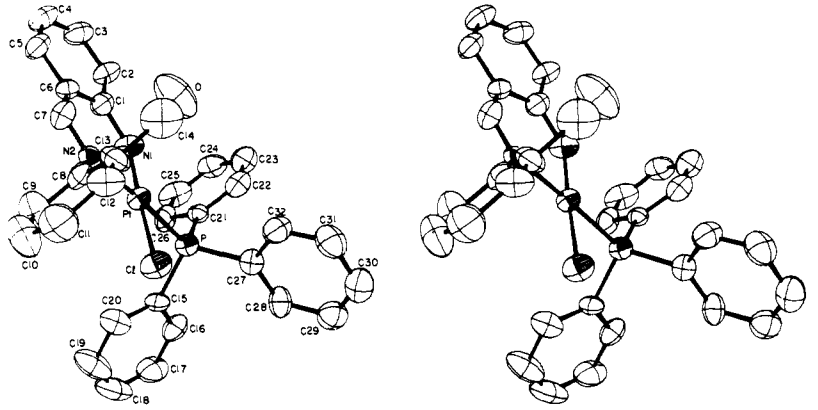

Figure 1. Stereoview of Pt(AAA)(PPh_3)Cl showing ellipsoids of 50% probability.

a primary amine. Intermediates have been isolated and characterized in several Schiff base condensations and have provided insight to the mechanisms in these systems. Various condensates of acetone with metal amines have been reported,[1-11] as well as dicarbinolamines from the condensation of 2,6-diformylpyridine and amines.[12] Recently, in this laboratory, a dimeric condensate was isolated in the tetramerization of *o*-aminobenzaldehyde in the presence of platinum(II) ion.[13]

The chemistry of the tridentate, dimeric condensate, obtained as a platinum(II) complex, Pt(AAA)Cl (**1**), may provide additional insight to pathways in the mechanisms of template condensations. In coordinating solvents a solvolysis occurs in which the aldehyde is displaced by solvent. For dimethyl sulfoxide and acetonitrile the process is reversible, whereby the coordinated solvent is expelled by irradiation of the complex with light in the visible region[14] (eq 1).

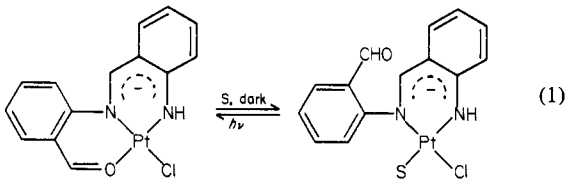

(1)

Pt(AAA)Cl S = coordinating solvent

1

The orientation of the liberated aldehyde is of interest because of possible weak association with the platinum via either the oxygen atom or a π-bonded complex. The latter has been postulated as an intermediate in metal ion activation of formyl groups.[15] Attempts to isolate a crystalline solvolysis product have thus far proven unsuccessful. In an effort to trap the uncoordinated aldehyde in an isolable crystalline form, a neutral (in order to maintain complex neutrality), strong field ligand, triphenylphosphine, was allowed to react with the platinum complex of the dimeric condensate. The infrared spectrum of the resulting deep-red crystalline product revealed the presence of the uncoordinated aldehyde. The results of the crystal structure determination of the triphenylphosphine adduct, Pt(AAA)(PPh_3)Cl, are reported herein.

Table I. Summary of Crystal Data for Pt(AAA)(PPh_3)Cl

formula	$PtClPON_2C_{32}H_{26}$
fw	716.09
cell parameters	
a, Å	32.75 (6)
b, Å	10.04 (2)
c, Å	19.71 (7)
β, deg	118.5 (2)
V, Å^3	5697 (25)
Z	8
ρ calcd (g cm^{-3})	1.668
ρ obsd (flotation, CH_2I_2/CCl_4, g cm^{-3})	1.70 (1)
space group	$C2/c$
cryst dimens, mm	0.20 × 0.20 × 0.40
temp, °C	25
radiatn	Mo Kα
μ, cm^{-1}	54.6
2θ range, deg	3.0–60.0
no. of independent reflections	3343
no. with $I > 3\sigma(I)$	2219
final R_1	0.043
final R_2	0.042

Experimental Section

Synthesis. All of the chemicals used were reagent grade with the exception of those used for spectral measurements, which were spectral grade. The preparation of the starting material, Pt(AAA)Cl, has been previously reported.[13] To prepare the triphenylphosphine adduct, a 1:1 molar ratio consisting of 0.030 g of Pt(AAA)Cl and 0.018 g of triphenylphosphine (0.068 mmol) was added to 100 mL of acetonitrile. The solution was stirred overnight in the dark at 35–40 °C. Upon slow evaporation of the acetonitrile, bright red crystals of Pt(AAA)(PPh_3)Cl were obtained and washed with chloroform. Anal. Calcd: N, 3.91; C, 53.67; H, 3.66. Found: N, 4.28; C, 53.98; H, 3.59.

Physical Measurements. Infrared spectra were recorded from 4000 to 400 cm^{-1} on a Perkin-Elmer Model 421 grating spectrophotometer as KBr pellets. Electronic spectra were obtained with 1-cm quartz cells on a Perkin-Elmer Model 555 UV-vis spectrophotometer in spectrograde acetonitrile. Elemental analyses for carbon, hydrogen, and nitrogen were performed at the Microanalytical Laboratory, University of Kansas, by Dr. Tho Nguyen.

X-ray Data. Single crystals of Pt(AAA)(PPh_3)Cl were obtained by slow evaporation of an acetonitrile solution of the complex. Preliminary measurements indicated monoclinic symmetry with systematic absences, hkl, $h + k \neq 2n$, and $h0l$, $l \neq 2n$. Successful refinement of the structure in the space group $C2/c$ confirmed it as the correct choice. Unit cell parameters were determined by an accurate centering of 15 reflections,[16] well distributed in reciprocal space. Crystal data information is

(1) Curtis, N. F. *J. Chem. Soc., Dalton Trans.* **1972**, 1357-61.
(2) Curtis, N. F. *J. Chem. Soc., Dalton Trans.* **1973**, 863-6.
(3) Cook, D. F.; Curtis, N. F. *J. Chem. Soc., Dalton Trans.* **1973**, 1076-9.
(4) Morgan, K. R.; Martin, J. W. L.; Curtis, N. F. *Aust. J. Chem.* **1979**, *32*, 2371-80.
(5) Hanic, F.; Serator, M. *Chem. Zvesti* **1964**, *18*, 572-83.
(6) Hanic, F.; Machajdik, D. *Chem. Zvesti* **1969**, *23*, 3-14.
(7) Domiano, P.; Musatti, A.; Pelizzi, C. *Cryst. Struct. Commun.* **1975**, *4*, 185-8.
(8) Goldberg, D. E. *J. Chem. Soc. A* **1968**, 2671-3.
(9) Jehn, W. *Z. Anorg. Allg. Chem.* **1967**, *351*, 260-7.
(10) House, D. A.; Curtis, N. F. *J. Am. Chem. Soc.* **1964**, *86*, 223-5.
(11) Black, D. St. C.; Greenland, H. *Aust. J. Chem.* **1972**, *25*, 1315-9.
(12) Hague, Z. P.; Tasker, P. A. Inorg. *Chem.* **1979**, *18*, 2920-1.
(13) Timken, M. D.; Sheldon, R. I.; Rohly, W. G.; Mertes, K. B. *J. Am. Chem. Soc.* **1980**, *102*, 4716-20.
(14) Rohly, W. G.; Mertes, K. B. *J. Am. Chem. Soc.* **1980**, *102*, 7939-40.
(15) Rauchfuss, T. B. *J. Am. Chem. Soc.* **1979**, *101*, 1045-7.
(16) "P2$_1$ Operations Manual"; Syntex Analytical Instrument Co.; Cupertino, CA, 1973.

Table II. Final Positional Parameters for Nonhydrogen Atoms in Pt(AAA)(PPh_3)Cl[a]

atom	x	y	z
Pt	0.11500 (2)	0.06595 (5)	−0.11485 (3)
Cl	0.0919 (1)	−0.1100 (3)	−0.2046 (2)
P	0.1386 (1)	0.1728 (3)	−0.1918 (2)
N(1)	0.1378 (3)	0.2130 (10)	−0.0368 (6)
N(2)	0.0901 (3)	−0.0320 (10)	−0.0495 (6)
O	0.1717 (4)	−0.1910 (13)	0.0375 (7)
C(1)	0.1353 (4)	0.2274 (13)	0.0298 (8)
C(2)	0.1595 (5)	0.3381 (12)	0.0813 (7)
C(3)	0.1548 (5)	0.3571 (15)	0.1464 (8)
C(4)	0.1275 (5)	0.2736 (15)	0.1668 (8)
C(5)	0.1052 (5)	0.1629 (15)	0.1190 (8)
C(6)	0.1091 (4)	0.1358 (14)	0.0520 (7)
C(7)	0.0890 (4)	0.0125 (13)	0.0120 (8)
C(8)	0.0694 (5)	−0.1667 (14)	−0.0740 (8)
C(9)	0.0218 (5)	−0.1749 (14)	−0.1248 (9)
C(10)	0.0017 (5)	−0.3008 (20)	−0.1519 (10)
C(11)	0.0281 (6)	−0.4154 (17)	−0.1299 (10)
C(12)	0.0760 (5)	−0.4093 (13)	−0.0765 (8)
C(13)	0.0968 (5)	−0.2837 (16)	−0.0492 (7)
C(14)	0.1462 (6)	−0.2853 (16)	0.0059 (10)
C(15)	0.0906 (4)	0.2300 (13)	−0.2842 (6)
C(16)	0.0454 (5)	0.1809 (13)	−0.3104 (8)
C(17)	0.0086 (5)	0.2191 (16)	−0.3805 (10)
C(18)	0.0161 (7)	0.3066 (20)	−0.4291 (9)
C(19)	0.0595 (7)	0.3589 (17)	−0.4048 (9)
C(20)	0.0971 (5)	0.3181 (15)	−0.3331 (8)
C(21)	0.1716 (4)	0.3292 (13)	−0.1488 (7)
C(22)	0.2195 (5)	0.3253 (14)	−0.1024 (8)
C(23)	0.2449 (5)	0.4405 (18)	−0.0650 (8)
C(24)	0.2219 (6)	0.5591 (18)	−0.0760 (8)
C(25)	0.1744 (7)	0.5690 (15)	−0.1249 (9)
C(26)	0.1474 (5)	0.4550 (15)	−0.1615 (8)
C(27)	0.1777 (4)	0.0724 (13)	−0.2137 (7)
C(28)	0.1844 (4)	0.0936 (13)	−0.2766 (8)
C(29)	0.2149 (5)	0.0154 (16)	−0.2913 (8)
C(30)	0.2406 (5)	−0.0849 (16)	−0.2393 (10)
C(31)	0.2353 (5)	−0.1069 (15)	−0.1740 (9)
C(32)	0.2050 (5)	−0.0274 (15)	−0.1604 (8)

[a] In this table and those subsequent, estimated standard deviations in the least significant figure are given in parentheses.

given in Table I. The data were collected as previously described.[17] Three reflections (2, 0, 2; 3, −1, 2; and 1, 1, 0), chosen as standards and monitored every 97 reflections, showed only random fluctuation over a 1.6% range. Lorentz and polarization factors were applied to obtain the structure factors.[18] Neither decay nor absorption corrections were applied. The F^2 values were brought to a relatively absolute scale by Wilson's method.

Solution and Refinement. The position of the platinum was ascertained from a Patterson map, and the positions of the remaining atoms were revealed by a subsequent Fourier map. Refinement was performed using full-matrix, least-squares techniques during which the function $\sum w(|F_o| - |F_c|)^2$ was minimized.[17] The data were weighted according to $1/\sigma_{F^2} = 4LpI/\sigma_I^2$. Refinement of positional and isotropic thermal parameters resulted in convergence at $R_1 = R_2 = 0.059$ where $R_1 = \sum||F_o| - |F_c||/\sum|F_o|$ and $R_2 = (\sum w(|F_o| - |F_c|)^2/\sum \omega|F_o|^2)^{1/2}$. At this point the thermal parameters were allowed to vary anisotropically, and hydrogen atom positions, calculated at a distance of 1.0 Å from the respective atoms and assigned thermal parameters 1 Å^2 greater than the isotropic B of the attached atom, were included as fixed contributions. Subsequent block-diagonal, least-squares refinement resulted in convergence at $R_1 = 0.042$ and $R_2 = 0.043$. In the final cycle of refinement no atom shifted by more than 0.03 of its esd. A final difference map was virtually featureless. Final positional parameters are listed in Table II. Atom numbering is shown in Figure 1, a stereoview of the molecule. Tables III and IV contain the calculated bond lengths and angles, respectively. Anisotropic thermal parameters, hydrogen atom positional and thermal parameters, and a list of observed and calculated structure factors are available as supplementary material.

Table III. Bond Lengths (Å) for Nonhydrogen Atoms in Pt(AAA)(PPh_3)Cl

Pt–Cl	2.355 (6)	P–C(15)	1.84 (1)
Pt–P	2.274 (6)	C(15)–C(16)	1.40 (2)
Pt–N(1)	2.00 (1)	C(16)–C(17)	1.38 (2)
Pt–N(2)	2.07 (1)	C(17)–C(18)	1.40 (2)
N(1)–C(1)	1.36 (2)	C(18)–C(19)	1.37 (2)
C(1)–C(2)	1.46 (2)	C(19)–C(20)	1.42 (2)
C(1)–C(6)	1.46 (2)	C(20)–C(15)	1.40 (2)
C(2)–C(3)	1.38 (2)	P–C(21)	1.86 (1)
C(3)–C(4)	1.42 (2)	C(21)–C(22)	1.39 (2)
C(4)–C(5)	1.41 (2)	C(22)–C(23)	1.41 (2)
C(5)–C(6)	1.41 (2)	C(23)–C(24)	1.37 (2)
C(6)–C(7)	1.45 (2)	C(24)–C(25)	1.39 (2)
C(7)–N(2)	1.31 (2)	C(25)–C(26)	1.42 (2)
N(2)–C(8)	1.49 (2)	C(26)–C(21)	1.45 (2)
C(8)–C(9)	1.40 (2)	P–C(27)	1.84 (1)
C(8)–C(13)	1.42 (2)	C(27)–C(28)	1.37 (2)
C(9)–C(10)	1.41 (2)	C(28)–C(29)	1.40 (2)
C(10)–C(11)	1.38 (2)	C(29)–C(30)	1.40 (2)
C(11)–C(12)	1.41 (2)	C(30)–C(31)	1.40 (2)
C(12)–C(13)	1.41 (2)	C(31)–C(32)	1.40 (2)
C(13)–C(14)	1.45 (2)	C(32)–C(27)	1.42 (2)
C(14)–O	1.22 (2)		

Results and Discussion

Both the infrared and visible spectra of the triphenylphosphine adduct show distinct similarities to those of the acetonitrile solvolysis product. A comparison of the infrared data for the two complexes and Pt(AAA)Cl in the region from 1700 to 1400 cm^{-1} is shown in Table V. The band at 1621 cm^{-1}, previously assigned to the carbonyl stretch in Pt(AAA)Cl, has disappeared and been replaced by a higher energy band in both adducts, attributed to the free aldehyde stretch. The bands in the region from 1620 to 1400 cm^{-1} can most probably be assigned to aromatic and conjugated ring interactions as in Pt(AAA)Cl.[13,19] In all three complexes an absorption occurs at approximately 1530 cm^{-1} and is assigned as the delocalized C⋯N stretch.[13,19] The evident differences in the adduct spectra in this region, compared to the spectrum of Pt(AAA)Cl, indicate possible differences in electron delocalization. Bands occurring at 1481 and 1435 cm^{-1} for the triphenylphosphine adduct are associated with triphenylphosphine vibrations. In the visible absorption spectrum of the triphenylphosphine adduct in acetonitrile as in the solvolyzed products of Pt(AAA)Cl, the intense absorption at 560 nm (ϵ 10000) has been replaced by a weaker band at 472 nm (ϵ 2500). In view of the intensity, it probably involves charge transfer or ligand transitions. The shift in wavelength and intensity may be a reflection of rotation of the anthranilaldehyde ring to a perpendicular orientation which prohibits any extension of electron delocalization from the *o*-aminobenzylidene ring. Unfortunately, because of the degree of uncertainty in the bond lengths as determined crystallographically, no definitive statement concerning differences in electron delocalization between Pt(AAA)Cl and the triphenylphosphine adduct can be made from the structural data.

Unlike the solvolysis products, the triphenylphosphine adduct does not show any photosensitivity in either the ultraviolet or visible wavelength regions. The similarity of the other physical aspects, namely, infrared and visible absorption spectra, to the photosensitive solvolysis products, however, render the triphenylphosphine adduct a suitable model for structural study.

The immediate coordination sphere of the platinum is square planar and consists of two nitrogen donor atoms from the *o*-aminobenzylidene ring, the chloride, and the phosphorus of the triphenylphosphine. As can be seen from the stereoview in Figure

(17) Mertes, K. B. *Inorg. Chem.* **1978**, *17*, 49–52.

(18) The programs used were local modifications of A. Zalkin's FORDAP for the Fourier summation, W. Busing, K. Martin, and H. Levy's ORFLS and ORFFE-II for least-squares and function and error calculations, and C. K. Johnson's ORTEP-II for the molecular structure drawing. Computations were performed on the Honeywell 66/60 computer at the University of Kansas. Scattering factors were obtained from Cromer D. T.; Waber, J. T. "International Tables for X-ray Crystallography"; Vol. IV; Kynoch Press: Birmingham, England, 1974; Table 2.2A. Anomalous dispersion corrections for platinum, chlorine, and phosphorus were obtained from Ibers, J. A. "International Tables for X-ray Crystallography", Vol. III; Kynoch Press: Birmingham, England, 1968; Table 3.3.2C.

(19) Melson, G. A.; Busch, D. H. *J. Am. Chem. Soc.* **1964**, *86*, 4837–7.

Table IV. Bond Angles (deg) for Pt(AAA)(PPh_3)Cl

N(1)-Pt-N(2)	89.2 (4)	Pt-P-C(15)	113.9 (5)
N(2)-Pt-Cl	91.8 (4)	P-C(15)-C(16)	120.5 (10)
Cl-Pt-P	86.7 (2)	C(15)-C(16)-C(17)	122.2 (14)
P-Pt-N(1)	92.5 (3)	C(16)-C(17)-C(18)	120.0 (15)
Pt-N(1)-C(1)	130.4 (9)	C(17)-C(18)-C(19)	119.4 (15)
N(1)-C(1)-C(2)	119.4 (12)	C(18)-C(19)-C(20)	120.0 (16)
N(1)-C(1)-C(6)	122.4 (12)	C(19)-C(20)-C(15)	121.6 (13)
C(6)-C(1)-C(2)	118.2 (12)	C(16)-C(15)-C(20)	116.6 (11)
C(1)-C(2)-C(3)	119.3 (12)	C(20)-C(15)-P	122.8 (10)
C(2)-C(3)-C(4)	123.3 (13)	C(15)-P-C(21)	102.8 (6)
C(3)-C(4)-C(5)	118.1 (12)	Pt-P-C(21)	113.7 (4)
C(4)-C(5)-C(6)	121.7 (13)	P-C(21)-C(22)	120.1 (10)
C(5)-C(6)-C(1)	119.2 (13)	C(21)-C(22)-C(23)	121.3 (12)
C(5)-C(6)-C(7)	117.1 (12)	C(22)-C(23)-C(24)	119.2 (13)
C(1)-C(6)-C(7)	123.6 (12)	C(23)-C(24)-C(25)	121.4 (14)
C(6)-C(7)-N(2)	126.2 (11)	C(24)-C(25)-C(26)	121.0 (14)
C(7)-N(2)-Pt	127.4 (9)	C(25)-C(26)-C(21)	117.4 (12)
C(7)-N(2)-C(8)	113.6 (10)	C(26)-C(21)-C(22)	119.4 (12)
Pt-N(2)-C(8)	119.0 (8)	C(26)-C(21)-P	120.4 (10)
N(2)-C(8)-C(9)	117.8 (12)	C(21)-P-C(27)	104.6 (6)
N(2)-C(8)-C(13)	121.7 (12)	Pt-P-C(27)	113.4 (5)
C(13)-C(8)-C(9)	120.4 (13)	P-C(27)-C(28)	123.9 (11)
C(8)-C(9)-C(10)	119.0 (14)	C(27)-C(28)-C(29)	117.6 (12)
C(9)-C(10)-C(11)	121.4 (14)	C(28)-C(29)-C(30)	119.3 (13)
C(10)-C(11)-C(12)	120.3 (14)	C(29)-C(30)-C(31)	119.7 (13)
C(11)-C(12)-C(13)	119.0 (13)	C(30)-C(31)-C(32)	119.9 (13)
C(12)-C(13)-C(8)	119.8 (12)	C(31)-C(32)-C(27)	121.0 (12)
C(12)-C(13)-C(14)	115.9 (14)	C(32)-C(27)-C(28)	117.6 (12)
C(8)-C(13)-C(14)	124.2 (14)	C(32)-C(27)-P	118.4 (10)
C(13)-C(14)-O	128.3 (15)	C(27)-P-C(15)	107.4 (6)

Table V. Infrared Spectral Data in the Region 1700–1400 cm^{-1} [a]

Pt(AAA) (PPh_3)Cl	Pt(AAA) (CH_3CN)Cl	Pt(AAA)Cl [b]	assignt
1697 vs	1692 vs	1621 vs	C=O
1615 vs	1615 vs	1592 s	aromatic and
1597 m	1594 m	1565 m	conjugated ring
1582 vs	1580 m	1546 m	interactions
1535 s	1530 s	1529 s	C⋯N
1480 s	1480 sh	1490 w	aromatic
1453 s	1460 m	1462 m	and conjugated
1435 s		1455 sh	ring interactions
		1439 m	
		1423 w	

[a] Abbreviations used: vs, very strong; s, strong; m, medium; w, weak; sh, shoulder. [b] Reference 13.

Table VI. Selected Mean Plane Calculations for Pt(AAA)(PPh_3)Cl

atom	displacement	atom	displacement
A. Pt-N(1)-N(2)-Cl-P			
$-0.739x + 0.438y - 0.511z = -2.279$			
Pt	0.002	Cl	−0.044
N(1)	−0.051	P	0.045
N(2)	0.048		
B. Pt-N(1)-C(1)-C(2)-C(3)-C(4)-C(5)-C(6)-C(7)-N(2)			
$-0.670x + 0.519y - 0.531z = -1.886$			
Pt	0.041	C(4)	0.032
N(1)	0.081	C(5)	0.083
C(1)	0.018	C(6)	0.050
C(2)	−0.084	C(7)	−0.036
C(3)	−0.072	N(2)	−0.114
C. N(2)-C(8)-C(9)-C(10)-C(11)-C(12)-C(13)-C(14)-O			
$0.642x + 0.068y - 0.764z = 2.780$			
N(2)	0.049	C(12)	0.013
C(8)	−0.009	C(13)	0.010
C(9)	−0.036	C(14)	−0.014
C(10)	−0.021	O	−0.021
C(11)	0.030		

1, the aldehyde is dissociated from the platinum with the benzaldehyde group poised perpendicularly to the *o*-aminobenzylidene ring. The angle of intersection of these two mean planes as reported in Table VI is 89.4°. The configuration of the parent compound is not retained as evidenced by the cis position of the phosphine with respect to N(1). Initial attack of the triphenylphosphine most probably does occur with retention of configuration, however, in view of the substantial mechanistic data for square-planar substitution reactions.[20] The congestion of a triphenylphosphine adjacent to the benzaldehyde group undoubtedly provides the impetus for isomerization to a sterically more favorable geometry. The orientation of the aldehyde oxygen deserves note as it is poised almost directly above N(2) [O-N(2)-C(7) = 93.8 (8)°, O-N(2)-C(8) = 80.7 (7)°, and O-N(2)-Pt = 96.0 (4)°] at a distance of 2.87 (1) Å, 0.18 Å less than the sum of the van der Waals radii.[21] Interestingly, the aldehyde has not rotated about the C(13)-C(14) bond to relieve the close contact with N(2). This evidently preferred oxygen orientation may be the result of weak electrostatic interactions of the oxygen with N(2) or possibly a packing restriction. There is virtually no platinum-oxygen interaction as evidenced by the long Pt-O distance of 3.72 (1) Å. As can be seen from the mean plane calculations in Table VI, the *o*-aminobenzylidene moiety, including the platinum, appears to be somewhat less planar than the anthranilaldehyde group. In both cases N(2) shows the largest deviation from the plane (0.11 Å in the former and 0.05 Å in the latter).

An examination of the platinum ligand bond lengths in Pt(AAA)Cl and the triphenylphosphine adduct reveals inherent differences which provide insight to the lability of the aldehyde. A comparison of relevant bond lengths and angles is shown in Figure 2. In Pt(AAA)Cl the Pt-N(1) and Pt-N(2) bond lengths differ significantly at 1.93 (2) and 1.99 (1) Å, the latter being the length more commonly associated with Pt(II)-N(chelate) distances.[22,23] The significantly shorter Pt-N(1) bond could derive in part from an increased nucleophilicity associated with the negatively charged terminal-NH^- function of the ligand as com-

(20) Wilkins, R. G. "The Study of Kinetics and Mechanism of Reactions of Transition Metal Complexes"; Allyn and Bacon: Boston, 1974; pp 223–235.
(21) Bondi, A. *J. Phys. Chem.* **1964**, *68*, 441–51.
(22) Jircitano, A. J.; Colton, M. C.; Mertes, K. B. *Inorg. Chem.* **1981**, *20*, 890–6.
(23) Phelps, D. W.; Little, W. F.; Hodgson, D. J. *Inorg. Chem.* **1976**, *15*, 2263–6.

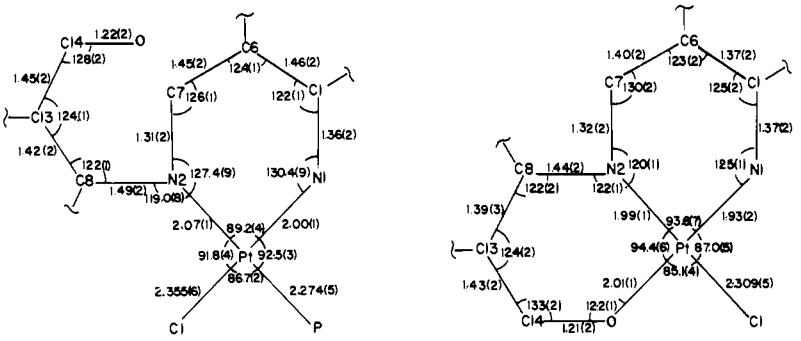

Figure 2. Comparison of bond lengths and angles for Pt(AAA)(Ph_3)Cl (on the left) and Pt(AAA)Cl[13] (on the right).

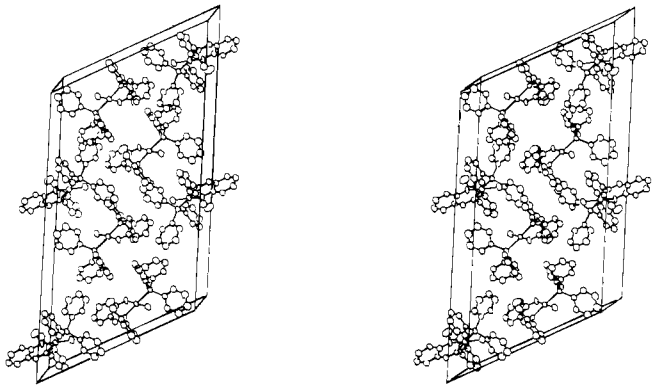

Figure 3. Packing diagram for Pt(AAA)(PPh_3)Cl as viewed down the *b* axis with the *a* axis vertical.

pared to a terminal neutral $-NH_2$ nitrogen. The result would be a strong trans effect emanating from the former moiety. Furthermore, the general tendency of the formyl group to coordinate to platinum(II) is not strong. In the bis complex of *o*-diphenylphosphinobenzaldehyde with platinum(II), for example, Rauchfuss has reported that the phosphine behaves as a monodentate ligand, coordinating through the phosphorus only.[15] A consideration of these two aspects, the strong trans-directing $-NH^-$ group as well as the weak tendency for platinum–formyl coordination, renders as highly predictable the observed lability of the aldehyde. Upon dissociation of the aldehyde, elongation of both Pt–N bonds is observed. The Pt–N(2) bond is distinctly longer at 2.07 (1) Å, undoubtedly a reflection of the strong trans influence of the triphenylphosphine. Pt–N(1) has also increased by 0.07 Å to 2.00 (1) Å, which can perhaps be attributed in part to the more strongly trans-directing chloride compared to the aldehyde. The absence of the bound aldehyde, the third "claw" of the chelate, may also affect bond lengthening by allowing for greater flexibility in the Pt–N bonds.

The electron delocalization in the *o*-aminobenzylidene ring is not as evident in the triphenylphosphine adduct as in Pt(AAA)Cl.[13] Primarily, it is observed only in the N(1)–C(1) bond of 1.36 (2) Å, which is distinctly shorter than the anticipated 1.48 (1) Å for R_2C-NH_2. C(1)–C(6) is significantly elongated compared to the analogous bond in Pt(AAA)Cl (1.46 (2) vs. 1.37 (2) Å), although no obvious explanation is discernible. Other bond lengths within the AAA rings are comparable with the previously reported structure. Unfortunately, subtle changes in the degree of electron delocalization cannot be ascertained from the current structural data.

The notable deviations in the chelate bond angles of the triphenylphosphine adduct compared to Pt(AAA)Cl involve a narrowing of the N(1)–Pt–N(2) angle from 93.6 (7) to 89.2 (4)° along with a widening of both Pt–N(2)–C(7) and Pt–N(1)–C(1) angles by 7 and 5°, respectively. The first could be a reflection of the increased flexibility of the bidentate vs. the tridentate chelate. Furthermore, the smaller angle could help to minimize repulsions between the bulky triphenylphosphine and N(1) on the one side and the pendant benzaldehyde ring with the coordinated aldehyde on the other. The widened inner ring angles at N(1) and N(2) are offshoots of the more acute ligand bite, while the other inner ring angles remain essentially unchanged.

Bond lengths and angles within the triphenylphosphine moiety are in agreement with other triphenylphosphine structures.[24] The molecular packing scheme is shown in Figure 3. In the parent Pt(AAA)Cl the near planarity of the complex allowed for the relatively close approach of the molecules (3.5 Å) which then could stack in an almost linear array.[13] In the adduct, however, the steric bulk of the triphenylphosphine, as well as the absence of planarity in the AAA ligand, makes close molecular approach sterically infeasible.

Still to be understood are the geometrical and electronic aspects of the photosensitivity of Pt(AAA)Cl. The synthesis and structure of related complexes are currently being investigated in order to elucidate the factors of influence in the chemistry and photochemistry.

Acknowledgment. K.B.M. acknowledges the donors of the Petroleum Research Fund, administered by the American Chemical Society, and the University of Kansas General Research Allocation No. 3229-XO-0038 for support of this research. Financial support from a National Science Foundation instrumentation grant for the purchase of the UV-vis spectrophotometer is also gratefully acknowledged.

Supplementary Material Available: Final thermal parameters for Pt(AAA)(PPh_3)Cl, positional and thermal parameters for H atoms, and structure factor tables (16 pages). Ordering information is given on any current masthead page.

(24) Strauss, S. H.; Diamond, S. E.; Mares, F.; Schriver, D. F. *Inorg. Chem.* **1978**, *17*, 3064–8.